

# Simplified Fermionic Scattering State Preparation for the NISQ Era

Michael Hite  
University of Iowa\*  
(Dated: May 2, 2025)

With quantum computers steadily improving, large volume quantum scattering simulations is getting very close. Yet, in the noisy intermediate scale quantum (NISQ) era, we are limited to shallow circuits on the order of a thousand layers. Thus, accurate and efficient state preparation methods are needed. We introduce a simplified fermionic scattering state preparation method that reduces circuit depth significantly by partially relaxing the fermionic condition. Using the 1+1D transverse field Ising model as our test bed with exact diagonalization and time evolving block decimation with matrix product states, we show that our simplified states retain nearly all of the behavior of the true fermionic state while being prepared on just a handful of qubits. We also show promising early results on IonQ Forte 1.

*Introduction* - Quantum computers provide a natural pathway for real-time scattering simulations, yet in the noisy intermediate scale quantum era (NISQ) [1], noise and qubit decoherence limit both simulation time and complexity. For digital computers which break up the simulation into a circuit of single and multi-qubit operations, this means that one must keep in mind gate execution times and system topology at all stages of the experiment (state preparation, time evolution, and measurement). For scattering simulations, much work has already been done in the development of techniques as well as promising results on present day hardware [2–12]. Jordan, Lee, and Preskill proposed a three step formulation for state preparation where one (1) prepares the ground state of the free theory, (2) excites wave packets from the ground state, and then (3) adiabatically evolves the state into the interacting theory [13, 14]. We will focus on step (2) in this work for the case of fermionic wave packets. The wave packets are a sum of fermionic creation operators. Via a Jordan-Wigner transformation, a fermionic creation operator acting on a site  $j$  is mapped to a product of Pauli-spin operators acting on qubits 0 to  $j - 1$ . Using standard decomposition procedures like Möttönen [15] or quantum Shannon [16], the wave packet preparation circuit has a couple hundred layers of two-qubit gates with just eight qubits, making it beyond the scope of what current hardware can do. Thus, efficient state preparation techniques are needed for the NISQ era. One technique which has shown great promise is decomposition using Given rotation matrices [17–19], which decomposes the state into a product of unitary particle conserving rotation operators. This has been used to simulate fermion/anti-fermion scattering in the Thirring Model [20]. Recent work has used scalable variational circuits and adapt-variational quantum eigensolver (VQE) to compose the wave packets [21, 22]. With the creation operators being non-unitary, Davoudi et. al [23] used ancillary qubits to place the operators in a larger unitary space to make wave packets for hadronic theories. Another way to approach this problem is by approximating the fermionic wave packets. In doing so, we seek to answer the question as to how much can we simplify the preparation without losing the majority behavior of the state? We propose a simplified wave packet preparation technique that localizes the state preparation operators in position space by partially relaxing the fermionic anti-commutation condition. In doing so, the depth of the circuit becomes independent of system size, only relying on the width of the individual wave packets. With the simplified preparation, we show that these packets retain much of the behavior of the true states, while allowing for straightforward tuning to increase accuracy.

This work is structured as follows. We will first introduce the transverse field Ising model and its fermionic mapping and then describe our simplified state preparation method. Then, using exact diagonalization and time evolving block decimation (TEBD) [24] with matrix product states (MPS), we verify that our simplification is a good approximation for the true fermionic state, and then show early results on IonQ Forte 1.

*Transverse Field Ising Model* - Consider an  $N$ -site transverse field Ising model in the basis where the transverse field is diagonal. The Hamiltonian for the system is given by

$$\hat{H} = - \sum_{j=1}^N (\lambda \hat{\sigma}_j^x \hat{\sigma}_{j+1}^x + \hat{\sigma}_j^z), \quad (1)$$

where  $\lambda$  is the nearest neighbor (transverse field) coupling constant, the coupling to the transverse field is set to one, and  $\sigma_{N+1} = \sigma_1$  for periodic boundary conditions. Diagonalization of the Hamiltonian requires three separate transformations: Jordan-Wigner, Fourier, and Bogoliubov [25–28]. We rely on the first two transformations. Introducing

---

\* mhite@uiowa.edu

Jordan-Wigner fermionic operators

$$\begin{aligned}\hat{c}_j^\dagger &= \left( \prod_{i=1}^{j-1} -\hat{\sigma}_i^z \right) \hat{\sigma}_j^-, \\ \hat{c}_j &= \left( \prod_{i=1}^{j-1} -\hat{\sigma}_i^z \right) \hat{\sigma}_j^+, \end{aligned} \quad (2)$$

where the product of  $\hat{\sigma}^z$ 's is called the Pauli string and assures the operators obey anti-commutation relations. The Hamiltonian in terms of these operators is

$$\hat{H} = \sum_{j=1}^N \left[ \lambda \left( \hat{c}_j^\dagger + \hat{c}_j \right) \left( \hat{c}_{j+1}^\dagger - \hat{c}_{j+1} \right) + 2 \left( \hat{c}_j^\dagger \hat{c}_j - 1 \right) \right], \quad (3)$$

such that  $\hat{c}_{N+1}^\dagger = \hat{c}_1^\dagger$ ,  $\hat{c}_{N+1} = \hat{c}_1$  for an odd number of particles, and  $\hat{c}_{N+1}^\dagger = -\hat{c}_1^\dagger$ ,  $\hat{c}_{N+1} = -\hat{c}_1$  for an even number of particles. In terms of momenta, this is accounted for by having separate momenta numbers for an odd and even number of particles:

$$k = \begin{cases} 0, \pm \frac{2\pi}{N}, \pm \frac{4\pi}{N}, \dots, \pm \frac{(N-2)\pi}{N}, \pi & (\text{odd}) \\ \pm \frac{\pi}{N}, \pm \frac{3\pi}{N}, \dots, \pm \frac{(N-1)\pi}{N} & (\text{even}) \end{cases}. \quad (4)$$

We'll denote the ground state as  $|\Omega\rangle$ . The Fourier operators, which we will use to do Fourier analysis are

$$\begin{aligned}\hat{\eta}_k^\dagger &= \frac{1}{\sqrt{N_s}} \sum_{j=1}^N e^{-ikj} \hat{c}_j^\dagger, \\ \hat{\eta}_k &= \frac{1}{\sqrt{N_s}} \sum_{j=1}^N e^{ikj} \hat{c}_j. \end{aligned} \quad (5)$$

In position space, a fermionic Gaussian wave packet centered at site  $x_0$  and momenta  $k_0$  is then

$$|\psi\rangle = \hat{\mathcal{G}}|\Omega\rangle = \sum_{j=1}^N e^{-ikx_j} e^{-r(x_0, x_j)^2 / \sigma^2} \hat{c}_j^\dagger |\Omega\rangle, \quad (6)$$

where  $r(x_0, x_j)$  is the distance between  $x_0$  and  $x_j$ , and  $\sigma$  is proportional to the width of the packet in position space.

*Mapping to a Quantum Computer* - If we consider the Gaussian wave packet operator we made in Equation 6, it is a sum of non-local Jordan-Wigner operators acting on the whole system. For an arbitrary  $M$ -qubit state, Mottonen decomposition would result in a circuit with at most  $2^{M+2} - 4M - 4$  CNOT gates and at a minimum  $\frac{1}{4}(2^{M+1} - 3M - 2)$  CNOT gates [15]. For eight sites, this would mean at most 988 CNOT gates and at a minimum 122 CNOT gates. Assuming these gates are only nearest neighbors, then we have at a maximum 247 CNOT layers and a minimum of around 30 CNOT layers. In practice with our states, we are usually at the maximum of CNOT layers. This is near the limit of what is possible with present day hardware, so we need a better way if we hope to do large volume calculations.

Suppose we choose  $\sigma$  such that the wave packet has a width of five qubits and is centered on qubit  $x_0$ . This means the only significant contributions to the sum will be from sites  $x_0 - 2, x_0 - 1, x_0, x_0 + 1$  and  $x_0 + 2$ . We can (1) truncate the sum to just these five terms. Yet, the operator is still a sum of multi-qubit operators ranging from qubits 0 to  $x_0 + 2$ . Thus, we need another way to localize the operators. This is accomplished by (2) cutting off the Pauli strings to the region of the packet, so

$$\begin{aligned}\hat{c}_{x_0-2}^\dagger &\longrightarrow \hat{\sigma}_{x_0-2}^-, \\ \hat{c}_{x_0-1}^\dagger &\longrightarrow -\hat{\sigma}_{x_0-2}^z \hat{\sigma}_{x_0-1}^-, \\ \hat{c}_{x_0}^\dagger &\longrightarrow \hat{\sigma}_{x_0-2}^z \hat{\sigma}_{x_0-1}^z \hat{\sigma}_{x_0}^-, \\ \hat{c}_{x_0+1}^\dagger &\longrightarrow -\hat{\sigma}_{x_0-2}^z \hat{\sigma}_{x_0-1}^z \hat{\sigma}_{x_0}^z \hat{\sigma}_{x_0+1}^-, \\ \hat{c}_{x_0+2}^\dagger &\longrightarrow \hat{\sigma}_{x_0-2}^z \hat{\sigma}_{x_0-1}^z \hat{\sigma}_{x_0}^z \hat{\sigma}_{x_0+1}^z \hat{\sigma}_{x_0+2}^-. \end{aligned} \quad (7)$$

For a single wave packet this is exact up to the truncated sum (step 1) if the Hamiltonian is translationally invariant. The same is not true for two wave packets. Consider two wave packets built in separate five qubit subspaces. If we have one packet centered at site 3, and the other at site 9, then

$$\{\hat{c}_j^\dagger, \hat{c}_{j'}^\dagger\} \neq 0 \quad (8)$$

for  $j \in \{1, 2, 3, 4, 5\}$  and  $j' \in \{7, 8, 9, 10, 11\}$ . This is due to the second set of Jordan strings not extending back to the origin. This may have a larger impact for certain observables more than others, so we must choose wisely what quantities to measure. Nevertheless, we now have two operators localized on sites 1-5 and 7-11 respectively. With this simplification, we can use Möttönen decomposition in these subspaces. If the wave packets are three qubits wide, then the number of CNOT layers is 4, and for packet of five qubits wide, the number of CNOT layers is only 26. This is substantially less than for the full state. In position space, we will measure the occupation number, which written in terms of Pauli-operators is

$$\hat{N}_j = \frac{1}{2} (1 - \hat{\sigma}_j^z). \quad (9)$$

We can also do Fourier analysis, where we measure the probability the state  $|\psi\rangle$  has momentum  $k$ :

$$\mathcal{P}(|k\rangle) = |\langle k|\psi\rangle|^2 \quad (10)$$

for

$$|k\rangle = \hat{\eta}_k^\dagger |\Omega\rangle. \quad (11)$$

We will use the full definition of  $\hat{\eta}_k^\dagger$  in Equation 5 with exact  $c^\dagger$ 's. Finally, to induce an interaction in the two particle sector, we will add the nearest neighbor term

$$\hat{H}' = \epsilon \sum_j \hat{\sigma}_j^z \hat{\sigma}_{j+1}^z, \quad (12)$$

for  $\epsilon > 0$  [11]. This will allow us to compare how our simplified wave packets interact to the exact wave packets.

*Compare with Exact and MPS Methods* - For a narrow wave packet (small  $\sigma$ ), there will be minimal difference between the full wave packet and the wave packet with truncated sum (step 1). So, in the following results, we work with  $\sigma$  such that the difference between the full and truncated state is minimal while still being reasonable. With the truncated sum, the operator still satisfies anti-commutation relations, so we will compare our approximate wave packets (two-fold simplification) to the truncated wave packets (only step 1). In an 8-site space, we generate a wave packet at site 1 with momenta center  $+\frac{3\pi}{8}$  and site 5 with momenta center  $-\frac{3\pi}{8}$ , both with width  $\sigma = \frac{3}{2}$ . In terms of qubits, each wave packet is three qubits wide. Figure 1 compares the initial state in both position and momentum space for the truncated and approximated wave packet. We see excellent agreement, especially in position space. Figure 2 (a) shows the evolution of the scattering state. If we consider all values of exact diagonalization such that  $\langle N_j(t) \rangle > 0.01$ , then the average percent error between the truncated and approximate state is 5.95%. We choose  $\langle N_j(t) \rangle > 0.01$  so near zero occupations are not unfairly weighted in the average. Figure 2 (c) shows the evolution of the momentum channel  $|+k, -k\rangle$  for  $k = 3\pi/8$  when the interacting term (Equation 12) is added with  $\epsilon = 0.1$ . We chose this channel as it was a maximum for the initial state, and we see an average percent error of only 1.71% from the truncated state. Increasing  $\epsilon$  to 0.3, percent error only rises to 2.79%. We expect the error to increase with increased  $\epsilon$  as it misses some of the fermionic interactions.

When going to larger spaces, we can widen the wave packets to five qubits each. In a 32 site system, we generate a wave packet at site 10 with momenta center  $+\frac{9\pi}{32}$  and one at site 20 with momenta center  $+\frac{9\pi}{32}$ . Both have  $\sigma = \frac{3}{2}$  and the nearest neighbor coupling is  $\lambda = 0.4$ . Figure 3 shows the evolution of the state using TEBD with Julia's ITensor library [29, 30], along with a comparison to the truncated case. If we consider all values of  $\langle N_j(t) \rangle > 0.005$ , then the average percent error is only 2.55% from the truncated state. The oscillations on site 32 we are exploring, as it should not be active throughout the evolution.

Now we would like to see the effect for introducing an interaction term. For one-dimensional scattering, we are often interested in finding the time delay and phase shift. In the one particle sector, an interaction capable of producing a time delay is a potential bump or well before an infinite wall. One can measure the time delay in the reflection coefficient of the incident wave to then get the phase shift. This has been done accurately with IBM hardware [11, 12]. Roughly, Equation 12 induces an interaction in the two particle sector. To measure the effect, we will work just with the occupation numbers. Take our 8-site example above. Site one has maximal occupation at  $t = 0$  and when the left

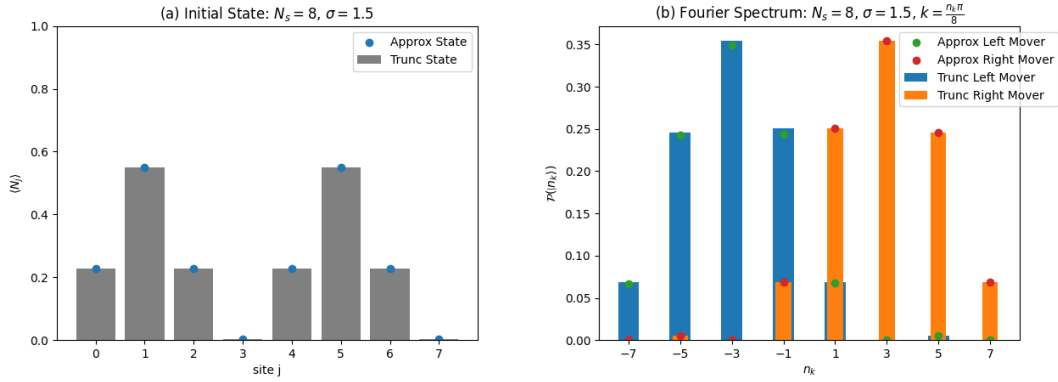


FIG. 1. Initial state in (a) position and (b) momentum space for a two packet truncated and approximate state.

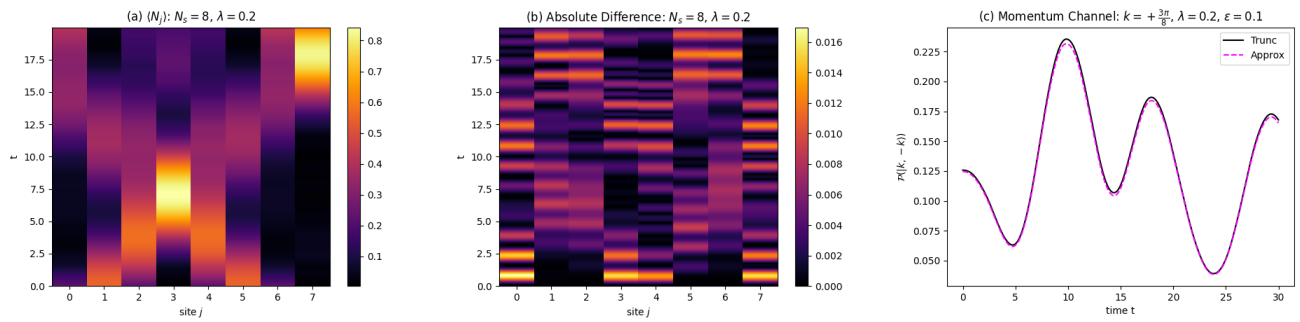


FIG. 2. (a) Evolution of the approximate initial state in Figure 1, (b) comparing to (absolute difference) the truncated state. (c) shows the evolution of the momentum channel  $| + k, -k \rangle$  for  $k = 3\pi/8$  when an interacting term with  $\epsilon = 0.1$  is turned on.

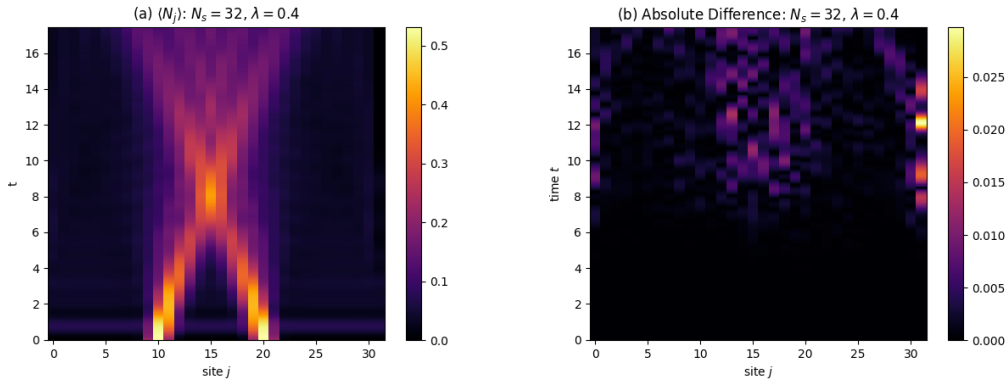


FIG. 3. (a) Evolution of a 32 site approximate initial state, (b) comparing to (absolute difference) the truncated state with TEBD.

moving wave packet passes through after the collision. With an interaction, the second time will be different than the free theory. To show scalability, we will go up to 32 sites, with a similar setup to Figure 3 where the wave packets are now 7 sites wide,  $\lambda = 0.2$ , and  $\Delta t = 0.08$ . The overlap occurs around  $t = 10$  and ends around  $t = 20$ . Figure 4 shows that initially there is no effect due to the interaction term but as the packet's overlap the interaction does indeed effect the evolution of the state. Nevertheless, our simplification does very well at capturing the time delay.

*Results with IonQ* - Now that we have verified that we have a good simplification for a fermionic wave packet scattering state, we show early simulations on IonQ Forte 1, a 36 qubit trapped ion machine with all-to-all connectivity. We generate the 8-qubit initial state Figure 1 (a) with 300 shots. Figure 5 (b) shows the evolution of the state with 275 shots. No error correction or mitigation procedures were used. Even with so few shots, the machine does very

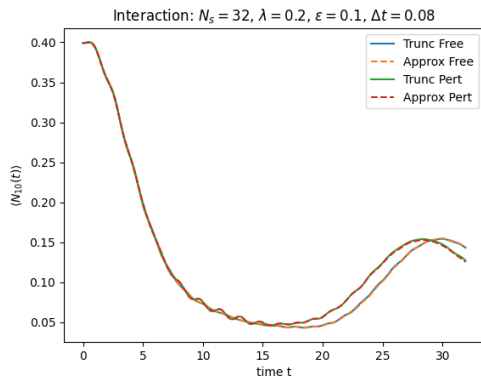


FIG. 4. Evolution of  $\langle N_{10}(t) \rangle$  for a two packet state in a 32 site space. The right moving wave packet is initialized at site 10.

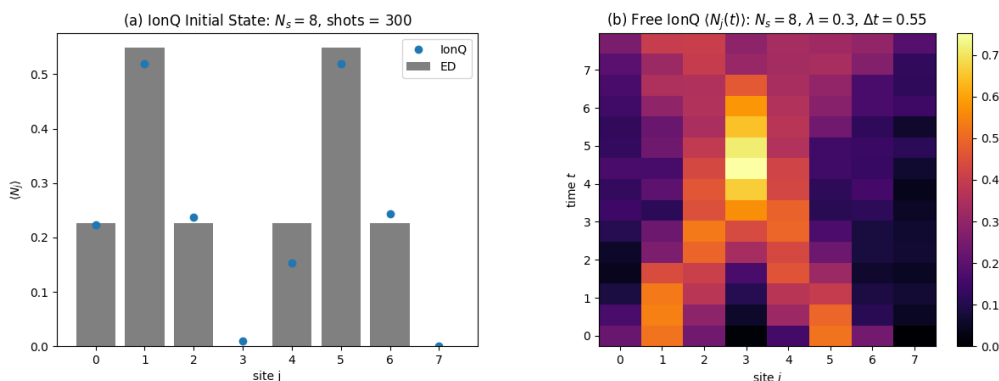


FIG. 5. (a) Initial state and (b) evolution of a simplified two packet scattering state in an 8-site system on IonQ Forte 1 QPU. The evolution was run with 275 shots and no error or noise correction was used.

well at preparing and evolving the state. We include this as a proof of concept for further investigation.

*Conclusion* - We have developed a simplified fermionic scattering state preparation for NISQ era quantum computing that dramatically reduces circuit depth by localizing the wave packet in space with the only drawback being a partial relaxation of fermionic condition. We showed that the simplified scattering states are very close to the true states in position and momentum space, and scale well for increased system size and with the addition of an interaction. Early results on IonQ Forte 1 show the machine can accurately produce the state with a limited number of shots. Future work will include a detailed analysis of truncating away terms of the Gaussian sum and cutting off Pauli strings, and runs on IonQ and IBM with an increased number of shots and noise correction and mitigation procedures. In doing so, we can compare resiliency between trapped ion and transmon qubit machines. Further, we can compare with traditional techniques like preparation using Givens rotations, and even exchange Möttönen decomposition for a Givens rotation decomposition in our method further reducing circuit depth. We expect this simplification procedure to be extremely beneficial for scattering simulations on near term quantum hardware.

*Acknowledgments* - This work is supported in part by the Department of Energy under Award Numbers DE-SC0019139 and DE-SC0010113 and NSF award DMR-1747426. We would like to thank Yannick Meurice, Muhammad Asaduzzaman, Cameron Cogburn and Zheyue Hang for intriguing and helpful discussions. We also thank Nikita Zemlevskiy for helpful comments on the manuscript.

- 
- [1] J. Preskill, Quantum Computing in the NISQ era and beyond, *Quantum* **2**, 79 (2018).  
 [2] M. Turco, G. Quinta, J. Seixas, and Y. Omar, Quantum simulation of bound state scattering, *PRX Quantum* **5**, 10.1103/prxquantum.5.020311 (2024).  
 [3] M. Kreshchuk, J. P. Vary, and P. J. Love, Simulating scattering of composite particles (2023), arXiv:2310.13742 [quant-ph].

- [4] R. A. Briceño, R. G. Edwards, M. Eaton, C. González-Arciniegas, O. Pfister, and G. Siopsis, Toward coherent quantum computation of scattering amplitudes with a measurement-based photonic quantum processor (2023), arXiv:2312.12613 [quant-ph].
- [5] S. Sharma, T. Papenbrock, and L. Platter, Scattering phase shifts from a quantum computer, *Physical Review C* **109**, 10.1103/physrevc.109.1061001 (2024).
- [6] P. Wang, W. Du, W. Zuo, and J. P. Vary, Nuclear scattering via quantum computing, *Physical Review C* **109**, 10.1103/physrevc.109.064623 (2024).
- [7] E. R. Bennowitz, B. Ware, A. Schuckert, A. Lerose, F. M. Surace, R. Belyansky, W. Morong, D. Luo, A. De, K. S. Collins, O. Katz, C. Monroe, Z. Davoudi, and A. V. Gorshkov, Simulating meson scattering on spin quantum simulators (2024), arXiv:2403.07061 [quant-ph].
- [8] F. Turro, K. A. Wendt, S. Quaglioni, F. Pederiva, and A. Roggero, Evaluation of phase shifts for non-relativistic elastic scattering using quantum computers (2024), arXiv:2407.04155 [quant-ph].
- [9] M. Yusf, L. Gan, C. Moffat, and G. Rupak, Elastic scattering on a quantum computer (2024), arXiv:2406.09231 [nucl-th].
- [10] E. Gustafson, Y. Meurice, and J. Unmuth-Yockey, Quantum simulation of scattering in the quantum ising model, *Phys. Rev. D* **99**, 094503 (2019).
- [11] E. Gustafson, Y. Zhu, P. Dreher, N. M. Linke, and Y. Meurice, Real-time quantum calculations of phase shifts using wave packet time delays, *Phys. Rev. D* **104**, 054507 (2021).
- [12] Z. Parks, A. Carignan-Dugas, E. Gustafson, Y. Meurice, and P. Dreher, Applying nox error mitigation protocols to calculate real-time quantum field theory scattering phase shifts (2023), arXiv:2212.05333 [quant-ph].
- [13] S. P. Jordan, K. S. M. Lee, and J. Preskill, Quantum algorithms for quantum field theories, *Science* **336**, 1130–1133 (2012).
- [14] S. P. Jordan, K. S. M. Lee, and J. Preskill, Quantum algorithms for fermionic quantum field theories (2014), arXiv:1404.7115 [hep-th].
- [15] M. Mottonen, J. J. Vartiainen, V. Bergholm, and M. M. Salomaa, Transformation of quantum states using uniformly controlled rotations (2004), arXiv:quant-ph/0407010 [quant-ph].
- [16] V. Shende, S. Bullock, and I. Markov, Synthesis of quantum-logic circuits, *IEEE Transactions on Computer-Aided Design of Integrated Circuits and Systems* **25**, 1000–1010 (2006).
- [17] J. M. Arrazola, Givens rotations for quantum chemistry, [https://pennylane.ai/qml/demos/tutorial\\_givens\\_rotations](https://pennylane.ai/qml/demos/tutorial_givens_rotations) (2021), date Accessed: 2025-03-01.
- [18] J. M. Arrazola, O. Di Matteo, N. Quesada, S. Jahangiri, A. Delgado, and N. Killoran, Universal quantum circuits for quantum chemistry, *Quantum* **6**, 742 (2022).
- [19] P. K. Barkoutsos, J. F. Gonthier, I. Sokolov, N. Moll, G. Salis, A. Fuhrer, M. Ganzhorn, D. J. Egger, M. Troyer, A. Mezzacapo, S. Filipp, and I. Tavernelli, Quantum algorithms for electronic structure calculations: Particle-hole hamiltonian and optimized wave-function expansions, *Phys. Rev. A* **98**, 022322 (2018).
- [20] Y. Chai, A. Crippa, K. Jansen, S. Kühn, V. R. Pascuzzi, F. Tacchino, and I. Tavernelli, Fermionic wave packet scattering: a quantum computing approach (2024), arXiv:2312.02272 [quant-ph].
- [21] R. C. Farrell, M. Illa, A. N. Ciavarella, and M. J. Savage, Quantum simulations of hadron dynamics in the schwinger model using 112 qubits (2024), arXiv:2401.08044 [quant-ph].
- [22] N. A. Zemlevskiy, Scalable quantum simulations of scattering in scalar field theory on 120 qubits (2024), arXiv:2411.02486 [quant-ph].
- [23] Z. Davoudi, C.-C. Hsieh, and S. V. Kadam, Scattering wave packets of hadrons in gauge theories: Preparation on a quantum computer (2024), arXiv:2402.00840 [quant-ph].
- [24] G. Vidal, Efficient classical simulation of slightly entangled quantum computations, *Phys. Rev. Lett.* **91**, 147902 (2003).
- [25] T. D. Schultz, D. C. Mattis, and E. H. Lieb, Two-dimensional ising model as a soluble problem of many fermions, *Rev. Mod. Phys.* **36**, 856 (1964).
- [26] S. Sachdev, *Quantum Phase Transitions*, 2nd ed. (Cambridge University Press, 2011).
- [27] B. Kaufman, Crystal statistics. ii. partition function evaluated by spinor analysis, *Phys. Rev.* **76**, 1232 (1949).
- [28] A. Cervera-Lierta, Exact ising model simulation on a quantum computer, *Quantum* **2**, 114 (2018).
- [29] M. Fishman, S. R. White, and E. M. Stoudenmire, The ITensor Software Library for Tensor Network Calculations, *SciPost Phys. Codebases* , 4 (2022).
- [30] M. Fishman, S. R. White, and E. M. Stoudenmire, Codebase release 0.3 for ITensor, *SciPost Phys. Codebases* , 4 (2022).